Journal of Statistical Physics, Vol. 114, Nos. 5/6, March 2004 (© 2004)

Ground-State Entropy of $\pm J$ Ising Lattices by Monte Carlo Simulations

F. Romá,[1] F. Nieto,[1] E. E. Vogel,[2] and A. J. Ramirez-Pastor[1]

Received November 26, 2002; accepted October 7, 2003

An accurate numerical calculation of the ground-state entropy associated to two-dimensional $\pm J$ Ising lattices is presented. The method is based on the use of the thermodynamic integration method. Total energy is calculated by means of the Monte Carlo method. Then the entropy (or degeneracy) of a state of interest is obtained by using thermodynamic integration starting at a known reference state. Results for small sizes are compared to exact values obtained by exhaustive scanning of the entire ground-state manifold, which serves as a test for the reliability of the simulation model developed here. The close agreement between simulated and exact results for energy and remnant entropy supports the validity of the technique used for describing the properties of $\pm J$ Ising lattices at the fundamental level. Finally, the results are extrapolated in order to estimate tendencies for larger systems.

KEY WORDS: Remnant entropy; thermodynamic integration; Monte Carlo method; $\pm J$ Hamiltonian; frustration.

1. INTRODUCTION

In many complex systems, evaluation of thermodynamic properties is a difficult matter. In the case of $\pm J$ Ising lattices it is even more so, due to the highly degenerate fundamental level as a consequence of two factors: (i) *frustration* and (ii) *randomness*.[1, 2] An analytic exact solution yielding the low-energy portion of the density of states (to mention just one example) is nearly impossible. Then it is necessary to shift to precise numerical calculations in order to calculate thermodynamic quantities such

[1] Department of Physics, Universidad Nacional de San Luis, CONICET, Chacabuco 917, 5700, San Luis, Argentina; e-mail: {froma, fnieto, antorami}@unsl.edu.ar

[2] Department of Physics, Universidad de La Frontera, Casilla 54-D, Temuco, Chile; e-mail: ee_vogel@ufro.cl

0022-4715/04/0300-1325/0 © 2004 Plenum Publishing Corporation

as free energy and entropy. However, the difficulty of reaching solutions of desired accuracy increases with lattice size. In the present paper, we aim to apply a method that leads to accurate descriptions of the just-mentioned thermodynamic variables for square lattices, even when temperature approaches zero and only states of the ground manifold (GM) are populated. For this extreme case, we have at our disposal exact results for small samples, which can be used for comparison to establish criteria to reach results of prescribed precision.

In fact, one difficult task in this work is to characterize the GM to calculate properties of these systems at extremely low temperatures. So far this has been done following two lines of thought: on one hand, exact calculations based on exhaustive scanning of the whole GM[3–7] and on the other hand, numerical techniques based on the analysis of a representative set of states belonging to the GM.[8–15] The number of states of the GM at the thermodynamic limit constitutes a very severe limitation for both descriptions. In fact, upon increasing the size of the system, the degeneracy of the GM grows exponentially. Thus, the huge computer time needed in either case makes these approaches nearly impossible.

Several authors have discussed the applicability of numerical algorithms for determining thermodynamic properties such as entropy. Without attempting a complete review of the field, let us mention here the attempt by S. Kirkpatrick[16] (among others) using Monte Carlo (MC) simulation techniques. Then, J. Vannimenus and G. Toulouse[17] made progress in the field taking advantage of the topological properties of the system. Some other authors, such as I. Morgenstern and K. Binder,[18] H.-F. Cheung and W. L. McMillan,[19] and A. J. Kolan and R. G. Palmer,[20] made important contributions using transfer matrix calculations. More recently, A. K. Hartmann[21] has explored the configuration space of these systems by means of a ballistic-search algorithm and genetic cluster-exact approximation (CEA). These diverse approaches have obtained different representative values for the entropy of the GM in the thermodynamic limit. In particular, in ref. 16 the evaluation of the remnant entropy has been determined via numerical implementation of the well-known "thermodynamic integration method" (TIM).[22] This pioneering work was one of the first reliable calculations of entropy associated to the GM. The disagreement between the numerical value proposed in that early work and those reported in more recent contributions can be attributed to the limited observation times used in the early work in comparison with the characteristic relaxation time scale of the phenomenon.

In this context, the main aim of the present work is to reformulate the use of the TIM and to show that it is able to determine accurate values for thermodynamic quantities associated to the GM of $\pm J$ Ising lattices. This

approach will be applied here to ground-state properties of two-dimensional (square) lattices. Even when absolute precision is lost, we will establish the main sources of error, thus making it possible to produce criteria for controlling accuracy. In particular, we address the following three issues: (a) testing the accuracy and correctness of our algorithms by comparing results with previous exact calculations for small lattice sizes;[3, 7] (b) establishing criteria to obtain reliable results for energy and entropy for larger systems; (c) formulating general conclusions about the applicability of this method to describe systems of larger size and higher dimensionality.

The article is organized as follows. In Section 2, the $\pm J$ Ising spin model is presented. The TIM procedure is described in Section 3, which also includes a discussion concerning numerical errors. In Section 4, we shall present results and discussions. Conclusions are summarized in Section 5.

2. ± J ISING LATTICES

Let us consider magnetic centers with two possible spin orientations sitting at the sites of a regular lattice interacting in pairs among nearest neighbors by means of interactions of mixed signs. This is the classical $\pm J$ Ising problem also known as the Edwards–Anderson $\pm J$ model.[1, 2, 23] We will focus on two-dimensional lattices, actually square lattices which are the most popular ones. However, extension to other geometries and higher dimensions should not represent formal problems. Such lattices have been studied very often as models for spin glasses,[2, 24, 25] and their connections extend to other branches of physics and statistical mechanics.[1] Competing interactions cannot be simultaneously satisfied, bringing in frustration. A frustrated bond is an exchange interaction contributing positively to the total energy of the system.

We shall describe these systems by means of the Ising Hamiltonian

$$H = \sum_{\langle j,k \rangle}^{N} J_{jk}\sigma_j\sigma_k, \tag{1}$$

where the sum runs over all pairs of nearest neighbors and all exchange interaction J_{jk} have the same magnitude J that can take the values $+1$ [antiferromagnetic (AF)] or -1 [ferromagnetic (F)]. The size of the lattice is represented by N, the total number of spins distributed in rectangular (eventually square) arrays. In particular, we restrict ourselves to equal concentration of AF and F interactions, which is not a limitation to the application of the TIM in any way. The actual distribution of N AF bonds and N F bonds will be done at random over $\frac{(2N)!}{N!^2}$ realizations to generate a

set of representative samples for each size. Each sample is a particular array of $\pm J$ interactions. σ_j represents the z component of spin at the jth site, which can be $+1$ or -1 for the sake of simplicity. Periodic boundary conditions are assumed to keep the coordination number constant through the lattice.

The complete solution for this Hamiltonian can be found by enumerating all the 2^N states (or 2^{N-1} due to the inversion symmetry of H). However, as has already been pointed out, such a method could need computer times that increase exponentially with N. Hence, the need for alternative methods relying on accuracy rather than completeness.

The ground-state energy is a magnitude that is size dependent. Thus, we will prefer to work with an intensive variable such as the ground-state energy per bond of each sample: $U_i(N)$ for the ith sample. Then the average GM energy can be given by

$$U_M(N) \equiv \langle U_i(N) \rangle; \tag{2}$$

the symbol $\langle \cdots \rangle$ is used here (and in the rest of this paper) to represent the average value of a magnitude over a set of M randomly generated samples of a given size.

Due to the combined effect of randomness and frustration, the GM is highly degenerated. For a given sample, the number of configurations with the same ground energy is $2W_i$ (an even number due to the above-mentioned inversion symmetry of the Hamiltonian). It is possible to define the GM entropy per bond for each sample as $S_i = \frac{\ln(2W_i)}{2N}$. For simplicity, we have used $k_B = 1$ throughout the text. Then, the GM average entropy per bond, $S_M(N)$, is given by

$$S_M(N) \equiv \langle S_i(N) \rangle. \tag{3}$$

3. THERMODYNAMIC INTEGRATION METHOD

3.1. Procedure

In order to calculate the entropy of a given sample (which is due to the density of states of the system), various methods have been developed.[26–32] Among them, the TIM is one of the most widely used and practically applicable.[22, 33–36] The method relies upon integration of the total energy as function of temperature along a reversible path. The initial point corresponds to an arbitrary but known reference state, while the final point corresponds to the state for which entropy is needed. Let us begin from the thermodynamic expression:

$$\frac{1}{T} = \left(\frac{\partial S}{\partial U} \right)_N, \tag{4}$$

where the system is characterized by its number of spins N at a temperature T with a total internal energy $U(N, T)$ and entropy $S(N, T)$. Denoting by t the dummy integration variable corresponding to temperature, we can now integrate Eq. (4) between two different equilibrium states, which leads to

$$S(N, T) - S(N, T_R) = \int_{U(T_R)}^{U(T)} \frac{dU}{t(N, U)}$$
$$= \frac{U(N, T)}{T} - \frac{U(N, T_R)}{T_R} - \int_{1/T_R}^{1/T} U(N, t)\, d\left(\frac{1}{t}\right). \quad (5)$$

In order to determine the numerical value of the entropy at an equilibrium thermodynamic state characterized by coordinates N and T, knowledge of the entropy for a reference thermodynamic state, $S(N, T_R)$, is required. In practice, calculation of $S(N, T_R)$ can present a severe restriction for many complex systems.[35, 36] Fortunately, for any Ising system comprising N spins, all its 2^N states are possible at infinite temperature, so entropy evaluated at $T_R \to \infty$ is trivially given by

$$\lim_{T_R \to \infty} S(N, T_R) = \ln 2^N. \quad (6)$$

Thus, according to Eqs. (5) and (6), for a particular sample GM entropy per bond can be obtained as:

$$S_i(N) = \frac{\ln 2^N}{2N} + \int_{\infty}^{0} U_i(N, t)\, d\left(\frac{1}{t}\right) = \frac{\ln 2}{2} + I_i(N). \quad (7)$$

The intermediate steps to reach this result are given in Appendix A.

Numerical evaluation of the integral $I_i(N)$ is the key element to finding the ground (remnant) entropy. To perform such an evaluation, we make use of two successive procedures: (a) MC simulation and (b) numerical integration technique.

MC simulation is used in this case to determine the average energy for n intermediate thermodynamic states between an initial condition ($T_R = \infty$) and a final one which we set at the GM ($T = 0$). This is illustrated in Fig. 1 for a particular sample containing $N = 16$ spins. Each point in the curve has been obtained by doing MC simulation based on Glauber's dynamics.[37] Thus, each spin is accessed randomly and the probability that it will flip is determined by the standard Metropolis algorithm.[38, 39] A Monte Carlo step (MCS) is equal to N such flip attempts. $r_o(N)$ MCSs are used to reach thermodynamic equilibrium at the temperature T, as will be

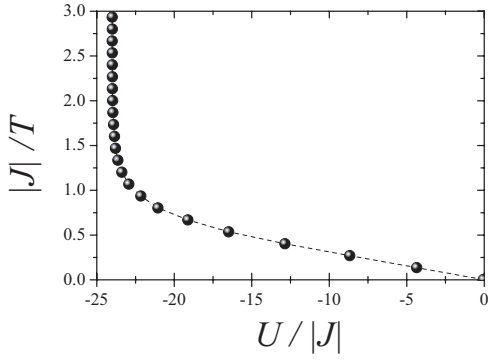

Fig. 1. $|J|/T$ versus the mean total energy per bond (in units of the interaction constant $|J|$) for the case $N = 16$. Simulations were carried out by using Glauber's dynamics. Symbols represent average values over typically 2×10^4 MC configurations, after reaching equilibration.

discussed in detail below. Then r additional MCSs are performed to obtain average values for the energy.

Once such a discrete curve formed by n points is obtained for a particular sample, numerical integration techniques are invoked to evaluate the RHS of Eq. (7). We used standard numerical algorithms to perform this integration.[40] Under these considerations, the values of entropy are affected with errors on both n and r. Due to the importance that such errors may have in the interpretation of our results, we discuss this matter in the next subsection.

3.2. Numerical Errors

Accuracy in the determination of the integral in Eq. (7) is improved if numerical errors are minimized. We review next the three main possible sources of error.

(a) Integration error (IE), which is derived from the numerical technique used for evaluation of the integral in Eq. (7).

(b) Simulation error (SE), which originates in the calculation of average energy for each sample at any T. This error is controlled by parameters r and N.

(c) Sampling error (SAE) associated to choosing the set of M representative samples for each N.

Let us now study each source of error separately. We will define below numerical constants A, B, C, and D, each one related to a different source

of error, so they will be evaluated by statistical methods applied to different distributions of numerical results. This analysis is done here for completeness so the role of each possible source of error is better understood.

The trapezoidal approximation technique[40] is widely used for numerical evaluation of integrals of continuous functions. Basically, an interval is divided into several segments. Thus, the integral of any function $f(x)$ defined in the interval $[a, b]$ can be written as

$$\int_a^b f(x)\,dx = \frac{h}{2}\left[f(a)+f(b)+2\sum_{l=1}^{n-1} f(x_l) \right] - \frac{(b-a)}{12} f''(\lambda)\, h^2, \tag{8}$$

where $h=(b-a)/n$ is the width of each segment, $x_l = a+hl$ is the beginning of the lth segment, λ is any point within the segment and $f''(\lambda)$ is the second derivative of f evaluated within the segment. The last term on the RHS of this equation is the systematic error in the process.

By using this methodology, the integral in Eq. (7) can be expressed as

$$I_i(N) = -\frac{2}{n}\left[U_i(N, T_0)+U_i(N, T_R)+2\sum_{l=1}^{n-1} U_i(N, T_l) \right] + \frac{16}{3n^2} U_i''(N, \tau), \tag{9}$$

where the integration interval has been defined between the limits $T_R = \infty$ ($b=0$) and $T_0 = 0.25$ ($a=4$), and τ is a point between these two cases. The lower limit, T_0, is the maximum value of temperature at which the finite system remains in the GM during the observation time (r).

Now, we rewrite Eq. (7) as

$$S_i(N) = \frac{\ln 2}{2} + I_i(N, r, n) + \frac{C}{n^2}, \tag{10}$$

where we recognize

$$I_i(N, r, n) = -\frac{2}{n}\left[U_i(N, T_0)+U_i(N, T_R)+2\sum_{l=1}^{n-1} U_i(N, T_l) \right] \tag{11}$$

and

$$C = \frac{16}{3} U_i''(N, \tau). \tag{12}$$

The third term on the RHS of Eq. (10) is the IE, which is a systematic error. Upon comparison of results obtained by using this expression with exact results available in the literature,[3, 7] it is found that C varies only slightly in the whole range of N considered here, which allows us to

determine a value $C \approx 2$ from now on. Then IE is only a function of parameter n, namely, IE $\propto n^{-2}$.

We shall focus now on the second term of Eq. (10), explicitly given in Eq. (11), which refers to energy. The error associated to the determination of the average energy, ΔU_i, can be estimated by the following expression:

$$\Delta U_i(N, T, r) = \frac{F_i(T)}{\sqrt{Nr}}. \tag{13}$$

As is well known,[41] the probability distribution for intensive variables of finite systems is given by a Gaussian function whose width is proportional to $N^{-1/2}$, which explains this factor in the previous equation. Similarly, the statistical dispersion of the variable over r MCSs provides the $r^{-1/2}$ dependence. Finally, we include a proportionality factor, $F_i(T)$, eventually dependent on temperature.

Following the same arguments, the error in the integral given by Eq. (10) is

$$\Delta I_i(N, r, n) = \frac{A_i}{\sqrt{Nrn}}, \tag{14}$$

where $A_i = \sqrt{8\langle F_i^2(T)\rangle_n}$. Here $\langle \cdots \rangle_n$ means average over the n results, one for each temperature of integration.

The previous treatment, as well as the one leading to the IE, represents the error for just one sample. By taking into consideration M samples for size N, we can write the following expression for average entropy:

$$S_M(N) = S_M(N, r, n) \pm \frac{A}{\sqrt{NrnM}} + \frac{C}{n^2}. \tag{15}$$

Here, $S_M(N, r, n) = \frac{\ln 2}{2} + \langle I_i(N, r, n)\rangle$ is the value obtained by MC simulations, in contrast with $S_M(N)$, which denotes the exact entropy value for the set of M samples under consideration. $A = \langle A_i \rangle$ is the average over M samples. A numerical estimation of constant A obtained after comparison with exact results allows us to report $A \approx 2$. The second term on the RHS of Eq. (15) is the SE.

Our final goal is to write down an expression for the average entropy $S(N)$ including all sources of error previously depicted. From the universe of all possible distributions of N F bonds plus N AF bonds, we have considered M samples at random. As the entropy per bond is an intensive variable, arguments used previously lead to

$$S(N) = S_M(N, r, n) \pm \frac{A}{\sqrt{NrnM}} \pm \frac{B}{\sqrt{NM}} + \frac{C}{n^2}, \tag{16}$$

where the term $B/\sqrt{NM}$ represents the SAE. After comparing exact and numerical results, it is found that $B \approx 0.14$.

Equation (16) allows us to choose the best set of parameters n, r, and M leading to accurate calculation of the entropy $S(N)$ according to the computation time available. This will be done in the next section.

4. RESULTS AND DISCUSSIONS

In this section, we report results for the physical quantities described in Section 2 using the methodology presented in the previous section. The calculation of total energy, energy fluctuations, correlation functions, etc. is rather straightforward by averaging over a large number of microscopic configurations of the system. However, entropy is much more difficult to evaluate. Moreover, an exact computation of remnant entropy requires an exhaustive scanning of the GM, which cannot be directly computed for fairly large lattices. Then, tackling the problem with reliable techniques to produce average values of magnitudes upon increasing size, keeping numerical errors under control, is a valid approximation. This can be even more important if the present analysis is extended to three-dimensional lattices.

The first quantity to be examined is the ground-state energy per bond as a function of size N, which is presented in Fig. 2, where we show the comparison between the present results obtained by the TIM (open triangles) and exact values obtained using the hierarchical scheme EFIS (represented by crosses). This last method is based on several numerical algorithms which improve performance, allowing one to reach exact results for ground-states of samples of intermediate size. The main stages of EFIS are: Expansion, which produces replicas of a seed random state to a total of N states so the Hamming distances are $N/2$ among all them (initialization of seed states continues until no new ground-states are found during a substantial number of such generations); Fall or descent, which minimizes the energy to reach a local minimum, so eventually a new ground-state is found; Invasion, which advances to all ground-states connected to previously found ground-states at no energy cost; Spring, which "jumps" by means of cellular automata from a set of interconnected ground-states to another set of interconnected ground-states, separated by energy barriers from the former. Interested readers are referred to ref. 7 for a more complete description of the algorithm EFIS.

It is important to note that for small sizes in Fig. 2 (N between 16 and 81) each point was calculated by using both methods separately on the same set of 500 samples for each size. The null error reported for the comparison between MC data and exact results means that the exact energy of

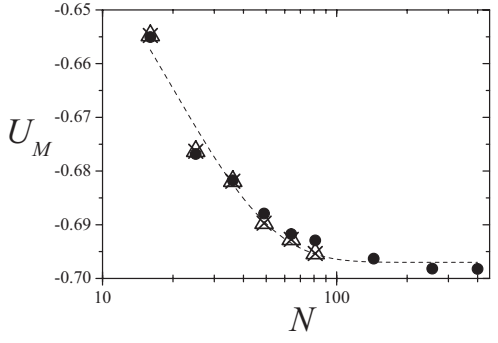

Fig. 2. GM energy per bond as a function of N, the number of spins in the lattice, comparing numerical results obtained by the TIM (open triangles) to exact results referred to in the text (crosses). Independently, data based on sets of 2000 samples per size (solid circles) represent the main result of the numerical simulations discussed in the text (a total of 18,000 independent samples were calculated to elaborate this figure). The dashed line is only a guide for the eye.

the GM was reached in the numerical treatment for each of the 3000 samples (considering the six sizes for which this comparison is possible at present). This exact match points to two important early conclusions to be used in the rest of this work: (a) MC simulations can produce exact values for ground-state energy if enough computer time is given; (b) in such a case, the only error in the evaluation of the average energy is associated with the set of representative samples. Then, by following same arguments used for other sources of errors in the previous section, we can write:

$$U(N) = U_M(N) \pm \frac{D}{\sqrt{NM}}, \tag{17}$$

where it is found that $D \approx 0.23$, as is obtained from the analysis of results corresponding to distributions over sets of samples of different sizes. The analysis of results of energy for larger samples (solid circles in Fig. 2) will be done later on after discussing the entropy for small samples.

One of the most crucial points to be elucidated in the spin-glass simulations is how to establish equilibration. This is even more important at low temperature as well as for increasing lattice sizes. In our study, the required r_o MCSs for recovering the exact results of entropy were calculated and stored for those values of N ranging from 16 to 81. For larger lattice sizes, equilibration times were estimated by extrapolating from the comparison with exact results. The accuracy and reliability of this extrapolation was

tested by increasing r_o by one order of magnitude without detecting any alteration in the results for a subset of samples of each size. With this criterion, r_o goes from 10^3 for $N = 16$ up to 10^6 for the largest lattices considered here, $N = 400$. As is expected, larger values of r_o are required upon increasing the lattice size. After equilibration, $r = 2 \times 10^4$ MCSs were used for averaging the desired quantities of interest.

Now we are ready to numerically calculate the entropy associated to the GM of systems under consideration. For sizes under $N = 81$, we use the same set of samples previously calculated by means of EFIS. According to the method discussed in Section 3, the entropy of the GM was obtained after numerical integration of the expression on the RHS of Eq. (7) with the following set of parameters: $n = 300$ and $r = 2 \times 10^4$. Figure 3 shows results of this procedure (open triangles) and those obtained via exact computation of the whole set of states of the GM done by EFIS (crosses). Direct comparison allows us to conclude that (a) the average error can be estimated as $\approx 10^{-5}$ and (b) for all considered sizes, MC average entropy resulted in a lower value as compared with the exact one. On the other hand, Eq. (15) predicts that the informed value of entropy is affected by an SE ($\approx \pm 10^{-6}$) and an IE ($\approx 10^{-5}$). It should be noted that the SE can be neglected in comparison with IE. Then we conclude that the two main sources of error lead to the same order of magnitude for systematic error (10^{-5}) affecting results produced by the MC data. This conclusion reinforces the validity of the arguments that accompanied the discussion leading to formulating Eq. (15).

It is clear that an accurate determination of asymptotic values for U and S in the thermodynamic limit requires going beyond $N = 81$. Therefore, the MC scheme emerges as a very important tool to reach this objective, expanding our capabilities for a deeper understanding of these systems.

Analysis thus far was based on the comparison between the TIM and EFIS for small sizes. After validating the TIM using exact results as a reference, we move on to grow in size with the aim of extracting general tendencies toward the thermodynamic limit. We prepared 2000 samples for each of the following sizes: 16, 25, 36, 49, 64, 81, 144, 256, and 400. In Fig. 2, we represent the values for $U_M(N)$ obtained by MC simulation (solid circles), using the same numerical values of parameters n and r already validated for smaller samples. From these numerical data, we have also extracted entropy $S_M(N)$ as a function of system size N. This is shown by solid circles in Fig. 3. In both illustrations, a monotonic decrease is clearly seen upon increasing size N. The reported values of energy $U(N)$ and entropy $S(N)$ for each size, with their respective errors, are collected in Table I. The main source of error in these data is associated with the SAE,

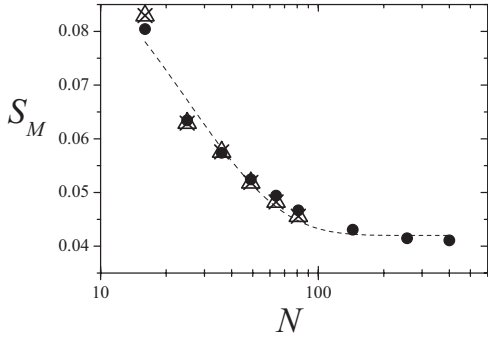

Fig. 3. GM remnant entropy per bond as a function of the number of spins in the lattice, N. Samples and symbols are the same as the corresponding ones in Fig. 2.

which is comparatively larger than all other types of error discussed here. SAE is tabulated in Table I as function of size. This is precisely the reason we increased to 2000 the number of samples per size for direct application of the TIM (solid circles in Figs. 2 and 3).

In order to determine the asymptotic limit for U and S, two strategies can be followed. The first one (not used here) assumes an empirical law for the size dependence of U and S using appropriate fitting parameters. The main disadvantage of this method is its strong dependence on the fitting law that determines the asymptotic value. Several authors have chosen a different technique,[16–21, 42] reporting the value of U and S for a large enough sample in order to minimize finite size effects. From now on, we follow this second strategy. From the analysis of Figs. 2 and 3 we can

Table I. Values for Energy U and Entropy S, with Their Corresponding Errors ΔU and ΔS, for the Different Sizes Reported in the Present Paper. $M = 2000$ Samples for Each Size Were Used in These Calculations

N	U	ΔU	S	ΔS
16	−0.6551	±0.0013	0.0804	±0.0008
25	−0.6768	±0.0010	0.0634	±0.0006
36	−0.6817	±0.0009	0.0574	±0.0005
49	−0.6879	±0.0007	0.0524	±0.0004
64	−0.6917	±0.0006	0.0494	±0.0004
81	−0.6929	±0.0006	0.0467	±0.0003
144	−0.6963	±0.0004	0.0431	±0.0003
256	−0.6982	±0.0003	0.0415	±0.0002
400	−0.6982	±0.0001	0.0409	±0.0001

conclude that the values of U and S stabilize for values of $N \approx 200$. Therefore, we have used the maximum size that our present computing capabilities allow, namely $N = 400$, using $n = 300$, $r = 2 \times 10^4$ and $M = 2000$, which ensures that the error is similar to the previous one. From the discussion above we can assume that the combined error is no larger than $O(10^{-4})$. Then we can report the following values for energy and entropy, with their corresponding errors, based on the analysis of samples 20×20:

$$U = -0.6982 \pm 0.0001, \tag{18}$$

$$S = 0.0409 \pm 0.0001. \tag{19}$$

Previous results compare well with those reported in the literature using different methodology. Thus, the most recent and exact value reported for energy is $U = -0.703$,[42] which is very close (less than 0.6% difference) to our result given above. Let us now move to a comparison of entropy, which is the core of our paper. In Table II we list results for the remnant entropy given in the literature, including in the last row our present results, which compare well with previous results. The advantage of a better and controlled accuracy can be appreciated. The spread of the different results of previous works reflects the difficulty of estimating the whole degeneracy of the GM by means of different numerical techniques. It should be noted that beyond the numerical agreement, the use of the TIM becomes validated in the context of the present approach. It is very interesting to note that our application of the TIM substantially improves the

Table II. Some of the Values for Remnant Entropy Reported in the Literature. The Last Row Corresponds to the Calculations Reported Here

Authors	S	Method	Lattice Size
Ref. 16 (1977)	0.050	TIM (low MCS's)	80×80
Ref. 17 (1977)	0.035	Mixed	20×20 to 30×30
Ref. 18 (1980)	0.037	Transfer Matrix	16×16
Ref. 20 (1982)	0.040†	Transfer Matrix	15×5 to 15×120
Ref. 19 (1983)	0.035	Transfer Matrix	Long strips of width from 3 up to 11
Ref. 21 (2001)	0.039	Ballistic-Search and CEA	20×20
Present paper	0.0409	TIM	20×20

† Estimated from the corresponding figure in ref. 20.

early results obtained by this method, yielding numbers that compare well with the rest of the proposals available in the literature.

5. CONCLUSIONS

In the present paper, we have discussed how the TIM can be used to determine the characteristic features of the ground-state properties of $\pm J$ Ising spin lattices. We have done simulations using a MC scheme to implement an algorithm capable of determining the energy and the entropy of the GM.

The applicability of the TIM has been tested and validated after a systematic study which established criteria to increase accuracy and to minimize sources of error. This was possible by comparing results of the TIM to exact values for the same variables obtained on the same set of samples of different sizes. By exact results we mean evaluation that is possible after complete scanning of the $2W$ states of the GM. Despite the fact that this calibration strategy can be used for small samples only, the generality of the treatment ensures good convergence for larger sizes. Nevertheless, for any extensive application of the TIM (as was done above for larger sizes, for instance) the method can be adapted to approach accurate results, identifying error sources and determining the corresponding error bars.

Average results for energy and remnant entropy coming exclusively from the TIM (solid circles in Figs. 2 and 3) not only compare well with average results for exact solutions on sets of samples, but they are also in good agreement with other calculations and general trends reported in the literature. Moreover, the error associated to our calculations is similar to or less than the error reported for other numerical calculations. The main source of error is the sampling error associated to a representative set of samples for each size. We have shown that 2000 randomly chosen samples provide a margin of error of less than 10^{-4}, which is good enough for comparison with previous results using alternative methods reported in the literature.

The strategy presented here for the analysis of $\pm J$ Ising spin lattices is a very promising one. Three possible lines of action point toward further applications of the TIM to present and other related systems: (1) to improve accuracy towards the thermodynamic limit of square and other two-dimensional lattices; (2) to help in the interpretation of the temperature evolution of several physical magnitudes (in particular, magnetic order parameters associated with the unfrustrated bonds in the $2W$ degenerated states of the GM) and (3) to extend this analysis to three-dimensional systems. These studies are in progress.

APPENDIX A

Let us begin with Eq. (5) in the main text, namely:

$$S(N,T)-S(N,T_R)=\frac{U(N,T)}{T}-\frac{U(N,T_R)}{T_R}-\int_{1/T_R}^{1/T}U(N,t)\,d\left(\frac{1}{t}\right). \tag{20}$$

If we write a Hamiltonian H' that differs from the original Hamiltonian H by a constant which will be denoted h, that is to say:

$$H'=H-h, \tag{21}$$

then,

$$U'(N,T)=U(N,T)-h. \tag{22}$$

Combining Eq. (20) and Eq. (22) we can write

$$\begin{aligned}S(N,T)-S(N,T_R)=&\frac{U'(N,T)}{T}+\frac{h}{T}-\frac{U'(N,T_R)}{T_R}-\frac{h}{T_R}\\&-\int_{1/T_R}^{1/T}U'(N,t)\,d\left(\frac{1}{t}\right)-h\int_{1/T_R}^{1/T}d\left(\frac{1}{t}\right).\end{aligned} \tag{23}$$

The last integral can be evaluated immediately leading to:

$$\begin{aligned}S(N,T)-S(N,T_R)=&\frac{U'(N,T)}{T}+\frac{h}{T}-\frac{U'(N,T_R)}{T_R}-\frac{h}{T_R}\\&-\int_{1/T_R}^{1/T}U'(N,t)\,d\left(\frac{1}{t}\right)-\frac{h}{T}+\frac{h}{T_R},\end{aligned} \tag{24}$$

which takes us back to an equation formally identical to the initial one, namely:

$$S(N,T)-S(N,T_R)=\frac{U'(N,T)}{T}-\frac{U'(N,T_R)}{T_R}-\int_{1/T_R}^{1/T}U'(N,t)\,d\left(\frac{1}{t}\right). \tag{25}$$

Previous analysis shows that an additive constant to the Hamiltonian does not alter the evaluation of entropy.

We now choose the ground-state energy as an additive constant such that

$$\lim_{T\to 0}U'(N,T)=\lim_{T\to 0}\left[U(N,T)-h\right]=0. \tag{26}$$

Under these circumstances, we want to determine the following limit:

$$\lim_{T\to 0} \frac{U'(N,T)}{T}, \tag{27}$$

which looks undefined at first glance. However, we can find such a limit after working with the partition function of the system. Namely:

$$Z = \sum_{i=0}^{\infty} g_i \exp\left[-\frac{H'_i}{T}\right], \tag{28}$$

where (a) this expression is evaluated in the thermodynamic limit (infinite number of states), (b) g_i and H'_i represent the degeneracy and energy of the ith level, respectively, and (c) $H'_o = 0$ (GM energy of the modified Hamiltonian).

The limit given by Eq. (27) is now written as

$$\lim_{T\to 0} \frac{U'(N,T)}{T} = \sum_{i=1}^{\infty} \frac{g_i H'_i}{g_o} \lim_{\beta\to\infty} \left\{\frac{\beta}{\exp[H'_i\beta]}\right\} \tag{29}$$

where $\beta = \frac{1}{T}$.

By using the L'Hopital theorem for evaluating the RHS limit, we obtain

$$\lim_{\beta\to\infty} \left\{\frac{\beta}{\exp[H'_i\beta]}\right\} = \lim_{\beta\to\infty} \left\{\frac{1}{H'_i\exp[H'_i\beta]}\right\} = 0 \qquad \text{for} \quad i > 0. \tag{30}$$

This result helps to go back to Eq. (7) in the main text.

ACKNOWLEDGMENTS

We thank Fondecyt (Chile) for support under projects 1020993 and 7020993. Three authors (FR, FN and AR) thank CONICET (Argentina) and Fundación Antorchas (Argentina) for partial support under project 13887-89. Two authors (F.R. and E.E.V.) thank the Millennium Scientific Initiative (Chile) under contract P02-054-F for partial support.

REFERENCES

1. K. Binder and A. P. Young, *Rev. Mod. Phys.* **58**:801 (1986).
2. M. Mezard, G. Parisi, and M. A. Virasoro, *Spin Glass Theory and Beyond* (World Scientific, Singapore, 1987).
3. E. E. Vogel, J. Cartes, S. Contreras, W. Lebrecht, and J. Villegas, *Phys. Rev. B* **49**:6018 (1994).

4. A. J. Ramirez-Pastor, F. Nieto, and E. E. Vogel, *Phys. Rev. B* **55**:14323 (1997).
5. E. E. Vogel, S. Contreras, M. A. Osorio, J. Cartes, F. Nieto, and A. J. Ramirez-Pastor, *Phys. Rev. B* **58**:8475 (1998).
6. A. J. Ramirez-Pastor, F. Nieto, S. Contreras, and E. E. Vogel, *Physica A* **283**:94 (2000).
7. A. J. Ramirez-Pastor, F. Nieto, and E. E. Vogel, *Physica A* **310**:384 (2002).
8. A. K. Hartmann, *Europhys. Lett.* **40**:429 (1997).
9. M. A. Moore, H. Bokil, and B. Drossel, *Phys. Rev. Lett.* **81**:4252 (1998).
10. M. Palassini and A. P. Young, *Phys. Rev. Lett.* **83**:5126 (1999).
11. K. F. Pál, *Physica A* **223**:283 (1996).
12. A. K. Hartmann, *Physica A* **224**:480 (1996).
13. A. K. Hartmann, *J. Phys. A: Math. Gen.* **33**:657 (2000).
14. Z. F. Zhan, L. W. Lee, and J.-S. Wang, *Physica A* **285**:239 (2000).
15. G. Hed, A. K. Hartmann, D. Stauffer, and E. Domany, *Phys. Rev. Lett.* **86**:3148 (2001).
16. S. Kirkpatrick, *Phys. Rev. B* **16**:4630 (1977).
17. J. Vannimenus and G. Toulouse, *J. Phys. C* **10**:L537 (1977).
18. I. Morgenstern and K. Binder, *Phys. Rev. B* **22**:288 (1980).
19. H.-F. Cheung and W. L. McMillan, *J. Phys. C* **16**:7027 (1983).
20. A. J. Kolan and R. G. Palmer, *J. Appl. Phys.* **53**:2198 (1982).
21. A. K. Hartmann, *Phys. Rev. E* **63**:016106 (2001).
22. K. Binder, The Monte Carlo method for the study of phase transitions: A review of some recent progress, *J. Comput. Phys.* **59**:1 (1985).
23. S. F. Edwards and P. W. Anderson, *J. Phys. F* **5**:965 (1975); G. Toulouse, *Commun. Phys.* **2**:115 (1977).
24. I. Morgenstern and K. Binder, *Phys. Rev. Lett.* **43**:1615 (1979).
25. K. H. Fisher and J. A. Hertz, *Spin Glasses*, Cambridge Studies in Magnetism I (Cambridge University Press, Cambridge, 1991).
26. Z. Salsburg, J. Jacobsen, W. Fickett, and W. Wood, *J. Chem. Phys.* **30**:65 (1959).
27. S. K. Ma, *J. Stat. Phys.* **26**:221 (1981).
28. Z. Alexandrowicz, *J. Chem. Phys.* **55**:2765 (1971).
29. H. Meirovitch, *Chem. Phys. Lett.* **45**:389 (1977).
30. C. H. Bennett, *J. Comput. Phys.* **22**:245 (1976).
31. J. P. Valleau and D. N. Card, *J. Chem. Phys.* **57**:5457 (1972).
32. G. Torrie and J. P. Valleau, *Chem. Phys. Lett.* **28**:578 (1974).
33. K. Binder, *J. Stat. Phys.* **24**:69 (1981); *Z. Phys. B* **45**:61 (1981).
34. T. L. Polgreen, *Phys. Rev. B* **29**:1468 (1984).
35. F. Romá, A. J. Ramirez-Pastor, and J. L. Riccardo, *Langmuir* **16**:9406 (2000).
36. F. Romá, A. J. Ramirez-Pastor, and J. L. Riccardo, *J. Chem. Phys.* **114**:10932 (2001).
37. K. Kawasaki, in *Phase Transitions and Critical Phenomena*, Vol. 2, C. Domb and M. Green, eds. (Academic, London, 1972).
38. N. Metropolis, A. W. Rosenbluth, M. N. Rosenbluth, A. H. Teller, and E. Teller, *J. Chem. Phys.* **21**:1087 (1953).
39. K. Binder, *Applications of the Monte Carlo Method in Statistical Physics. Topics in Current Physics,* Vol. 36 (Springer, Berlin, 1984), p. 23.
40. W. H. Press, S. A. Teukolsky, W. T. Vetterling, and B. P. Flannery, *Numerical Recipes in C++*, 2nd edn. (Cambridge University Press, London, 2002).
41. R. Brout, *Phys. Rev.* **115**:824 (1959).
42. R. G. Palmer and J. Adler, *Int. J. Mod. Phys. C* **10**:667 (1999).